January 9, 2014

Maximal CP nonconservation in the Two-Higgs-Doublet Model[1]

Wafaa Khater and Per Osland

Department of Physics, University of Bergen, Allegt. 55, N-5007 Bergen, Norway

Abstract

We study the simplest Two-Higgs-Doublet Model that allows for CP nonconservation, where it can be parametrized by only *one* parameter in the Higgs potential. Different concepts of *maximal* CP-nonconservation in the gauge-Higgs and the quark-Higgs (Yukawa) sectors are compared. Maximal CP nonconservation in the gauge-Higgs sector does normally not lead to maximal CP nonconservation in the Yukawa sector, and vice versa.

1 Introduction

Mendez and Pomarol introduced the concept of maximal CP nonconservation [1] in the context of the gauge–Higgs sector of the Two-Higgs-Doublet Model (2HDM) [2]. In the absence of CP nonconservation, only two of the three neutral Higgs bosons couple to the electroweak gauge bosons (the two CP even ones, often denoted h and H). When CP is *not* conserved, all three do. In fact, Mendez and Pomarol realized that the product of all three gauge–Higgs couplings, which is bounded by unitarity, is a useful concept to parametrize the amount of CP nonconservation, and defined the quantity

$$\xi_V = 27[g_{VVH_1}\, g_{VVH_2}\, g_{VVH_3}]^2 \tag{1.1}$$

[1]Invited talk given at the Cracow Epiphany conference on heavy flavours, 3 - 6 January 2003, Cracow, Poland. To be published in Acta Physica Polonica, July 2003.

as a measure of CP nonconservation in the gauge–Higgs sector. If the couplings g_{VVH_i} are normalized with respect to those of the Standard Model (SM), then ξ_V, as defined above, satisfies

$$0 \leq \xi_V \leq 1. \tag{1.2}$$

However, this measure of CP nonconservation is not applicable to the fermion–Higgs sector.

In the fermion–Higgs sector of a given version of the 2HDM, one should consider quantities other than ξ_V as measures of CP nonconservation. As we will see from our investigation, the parameters of the 2HDM that maximize ξ_V are *different* from those that maximize CP nonconservation in the Yukawa sector. They are in general also different for the up- and down-quark sectors.

The paper is organized as follows. In sect. 2 we review the 2HDM and in sect. 3 we study the conditions for maximum CP nonconservation in the gauge–Higgs sector. Sections 4 and 5 are devoted to the Yukawa sector, at the parton and proton level, respectively, and sect. 6 contains some concluding remarks.

2 The Two-Higgs-Doublet Model

We shall here introduce some notation for the Two-Higgs-Doublet Model [3]. Let the Higgs potential be parametrized as [4]

$$\begin{aligned} V &= \frac{\lambda_1}{2}(\phi_1^\dagger\phi_1)^2 + \frac{\lambda_2}{2}(\phi_2^\dagger\phi_2)^2 + \lambda_3(\phi_1^\dagger\phi_1)(\phi_2^\dagger\phi_2) + \lambda_4(\phi_1^\dagger\phi_2)(\phi_2^\dagger\phi_1) \\ &\quad + \frac{1}{2}\left[\lambda_5(\phi_1^\dagger\phi_2)^2 + \text{h.c.}\right] - \frac{1}{2}\left\{m_{11}^2(\phi_1^\dagger\phi_1) + \left[m_{12}^2(\phi_1^\dagger\phi_2) + \text{h.c.}\right] + m_{22}^2(\phi_2^\dagger\phi_2)\right\}. \end{aligned} \tag{2.1}$$

The parameters λ_5 and m_{12}^2 are allowed to be complex, subject to the constraint

$$\text{Im}\, m_{12}^2 = \text{Im}\, \lambda_5\, v_1 v_2, \tag{2.2}$$

with v_1 and v_2 the vacuum expectation values ($v_1^2 + v_2^2 = v^2$, with $v = 246$ GeV).

The corresponding neutral-Higgs mass matrix squared is then given by

$$\mathcal{M} = v^2 \begin{pmatrix} \lambda_1 c_\beta^2 + \nu s_\beta^2 & (\lambda_{345} - \nu) c_\beta s_\beta & -\frac{1}{2}\text{Im}\, \lambda_5\, s_\beta \\ (\lambda_{345} - \nu) c_\beta s_\beta & \lambda_2 s_\beta^2 + \nu c_\beta^2 & -\frac{1}{2}\text{Im}\, \lambda_5\, c_\beta \\ -\frac{1}{2}\text{Im}\, \lambda_5\, s_\beta & -\frac{1}{2}\text{Im}\, \lambda_5\, c_\beta & -\text{Re}\ \lambda_5 + \nu \end{pmatrix} \tag{2.3}$$

with the abbreviations $c_\beta = \cos\beta$, $s_\beta = \sin\beta$, $\tan\beta = v_2/v_1$, $\lambda_{345} = \lambda_3 + \lambda_4 + \mathrm{Re}\,\lambda_5$, $\nu = \mathrm{Re}\,m_{12}^2/(2v^2 \sin\beta\cos\beta)$ and $\mu^2 = v^2\nu$.

The $(1,3)$ and $(2,3)$ elements of this mass-squared matrix (2.3), which are responsible for CP nonconservation, are related via the angle β. In this sense, CP nonconservation is described by *one* parameter, namely $\mathrm{Im}\,\lambda_5$.

In order to diagonalize this matrix (2.3), we introduce the rotation matrix

$$\begin{aligned} R = R_c\, R_b\, R_{\tilde\alpha} &= \begin{pmatrix} 1 & 0 & 0 \\ 0 & \cos\alpha_c & \sin\alpha_c \\ 0 & -\sin\alpha_c & \cos\alpha_c \end{pmatrix} \begin{pmatrix} \cos\alpha_b & 0 & \sin\alpha_b \\ 0 & 1 & 0 \\ -\sin\alpha_b & 0 & \cos\alpha_b \end{pmatrix} \begin{pmatrix} \cos\tilde\alpha & \sin\tilde\alpha & 0 \\ -\sin\tilde\alpha & \cos\tilde\alpha & 0 \\ 0 & 0 & 1 \end{pmatrix} \\ &= \begin{pmatrix} c_{\tilde\alpha}\, c_b & s_{\tilde\alpha}\, c_b & s_b \\ -(c_{\tilde\alpha}\, s_b\, s_c + s_{\tilde\alpha}\, c_c) & c_{\tilde\alpha}\, c_c - s_{\tilde\alpha}\, s_b\, s_c & c_b\, s_c \\ -c_{\tilde\alpha}\, s_b\, c_c + s_{\tilde\alpha}\, s_c & -(c_{\tilde\alpha}\, s_c + s_{\tilde\alpha}\, s_b\, c_c) & c_b\, c_c \end{pmatrix} \end{aligned} \tag{2.4}$$

with $c_i = \cos\alpha_i$, $s_i = \sin\alpha_i$, and satisfying

$$R\mathcal{M}R^{\mathrm{T}} = \mathrm{diag}(M_1^2, M_2^2, M_3^2). \tag{2.5}$$

Here, $M_1 \le M_2 \le M_3$. The angular ranges are taken as $-\pi/2 < \tilde\alpha \le \pi/2$, $-\pi < \alpha_b \le \pi$, and $-\pi/2 < \alpha_c \le \pi/2$. As discussed in [5], only some regions of the parameter space are physically allowed.

This limitation of the parameter space is due to various constraints, including (i) $M_1 \le M_2 \le M_3$, and (ii) the constraints of perturbativity and unitarity. We shall represent the latter as

$$|\lambda_i| < 4\pi\,\xi_{\mathrm{pert}}, \quad \text{with } \xi_{\mathrm{pert}} = \mathcal{O}(1). \tag{2.6}$$

We show in Fig. 1 typical allowed regions in the α_b–α_c plane, for a few values of $\tan\beta$ and $\tilde\alpha$. In this figure, we only show regions of $|\alpha_b| \le \pi/2$ and only positive α_c. Regions of larger $|\alpha_b|$ and negative α_c are given by the symmetries discussed in [5]. Furthermore, for given values of $\tan\beta$ and $\tilde\alpha$ (and given sign of $\alpha_c > 0$), only *one sign* of α_b is realized, requiring $M_2 \le M_3$. The dashed lines at $\alpha_b = \pm\pi/4$ indicate where CP nonconservation is maximal in the Higgs–top-quark sector, in the limit of *one* light Higgs boson and two heavier ones, see Eq. (5.4).

Different choices for the 'soft parameters' (in particular, different values of μ^2) lead to somewhat different allowed regions. Also, a larger value of ξ_{pert} extends the region.

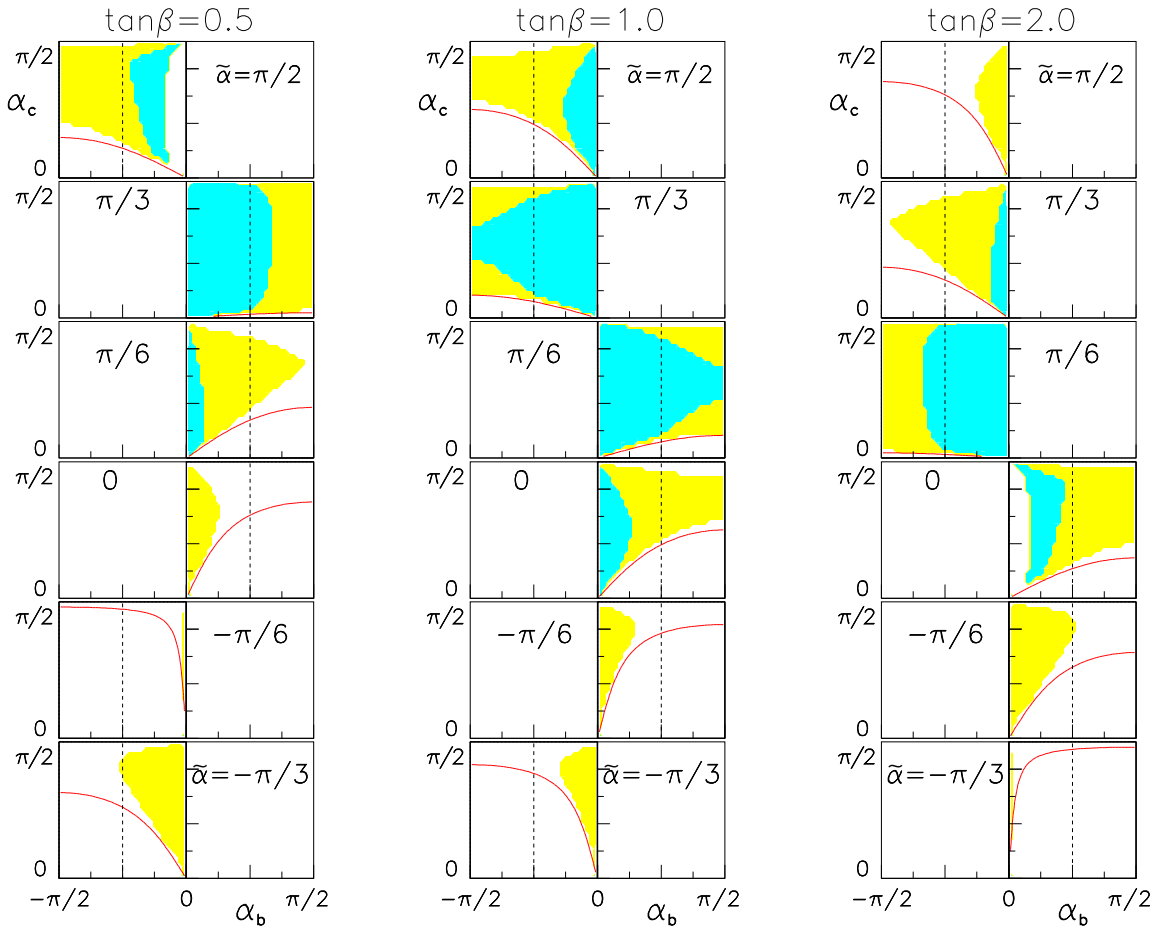

Figure 1: Dark (blue): physical regions [see Eq. (2.6)] in the α_b–α_c plane for various values of $\tan\beta$ and $\tilde{\alpha}$. Soft parameters: $M_1 = 100$ GeV, $M_2 = 500$ GeV, $M_{H^\pm} = 600$ GeV, $\mu = 300$ GeV, $\xi_{\rm pert} = 1$. Light (yellow): Same with $\xi_{\rm pert} = 5$. Solid contour: absolute boundary.

However, there are absolute bounds, indicated by the solid contours outside the shaded regions in Fig. 1, that can not be crossed for any choice of the 'soft parameters' [5]. In order to cover a range of different choices for μ^2, one may take a rather large value of $\xi_{\rm pert}$ (in sect. 5 we shall consider $\xi_{\rm pert} = 5$). For further discussion of these issues, see [5, 6].

In this notation, Eqs. (2.3)–(2.5), the gauge–Higgs couplings are, relative to the corresponding SM coupling, given by

$$H_i ZZ: \qquad g_{VVH_i} = \cos\beta\, R_{i1} + \sin\beta\, R_{i2}, \tag{2.7}$$

whereas for the Yukawa couplings we consider the so-called Model II [3] where they are

given by

$$H_j t\bar{t}: \qquad \frac{1}{\sin\beta}\,[R_{j2} - i\gamma_5 \cos\beta R_{j3}] \equiv [a_j^{(t)} + i\gamma_5 \tilde{a}_j^{(t)}], \tag{2.8}$$

$$H_j b\bar{b}: \qquad \frac{1}{\cos\beta}\,[R_{j1} - i\gamma_5 \sin\beta R_{j3}] \equiv [a_j^{(b)} + i\gamma_5 \tilde{a}_j^{(b)}], \tag{2.9}$$

with R_{ij} an element of the rotation matrix (2.4).

3 CP nonconservation in the gauge-Higgs sector

In the gauge–Higgs sector, the amount of CP nonconservation [cf. Eq. (1.1)] is in the above notation given by

$$\xi_V = 27 \prod_{i=1}^{3} [\cos\beta R_{i1} + \sin\beta R_{i2}]^2. \tag{3.1}$$

This ξ_V depends on $\tan\beta$ as well as on the three angles $\tilde{\alpha}$, α_b and α_c that determine R_{ij}. However, it only depends on β and $\tilde{\alpha}$ through their *difference*. In fact, using (2.4) and some trigonometric identities, we find

$$\xi_V = 27 c_b^2 \cos^2(\beta - \tilde{\alpha}) [s_b\, s_c \cos(\beta - \tilde{\alpha}) - c_c \sin(\beta - \tilde{\alpha})]^2 [s_b\, c_c \cos(\beta - \tilde{\alpha}) + s_c \sin(\beta - \tilde{\alpha})]^2. \tag{3.2}$$

It is also seen that ξ_V is unchanged under

$$\begin{aligned} &\alpha_b \text{ fixed}, \quad (\alpha_c \leftrightarrow \pi/2 + \alpha_c): && \xi_V \leftrightarrow \xi_V, \\ &(\alpha_b \leftrightarrow -\alpha_b), \quad (\alpha_c \leftrightarrow \pi/2 - \alpha_c): && \xi_V \leftrightarrow \xi_V. \end{aligned} \tag{3.3}$$

In order to provide some intuition for how the CP nonconservation depends on the parameters of the 2HDM, we show in Fig. 2 contours of constant ξ_V in the α_b–α_c plane, for various values of $\tan\beta$ and $\tilde{\alpha}$. We note that there is little CP nonconservation for 'large' values of α_b, because of the factor c_b^2 in (3.2). Also, there is CP nonconservation even for $\alpha_b = 0$ and for $\alpha_c = 0$ (but not when both vanish).

3.1 Simple limits

It is instructive to consider the simple limits of $\alpha_b = 0$ or $\alpha_c = 0$.

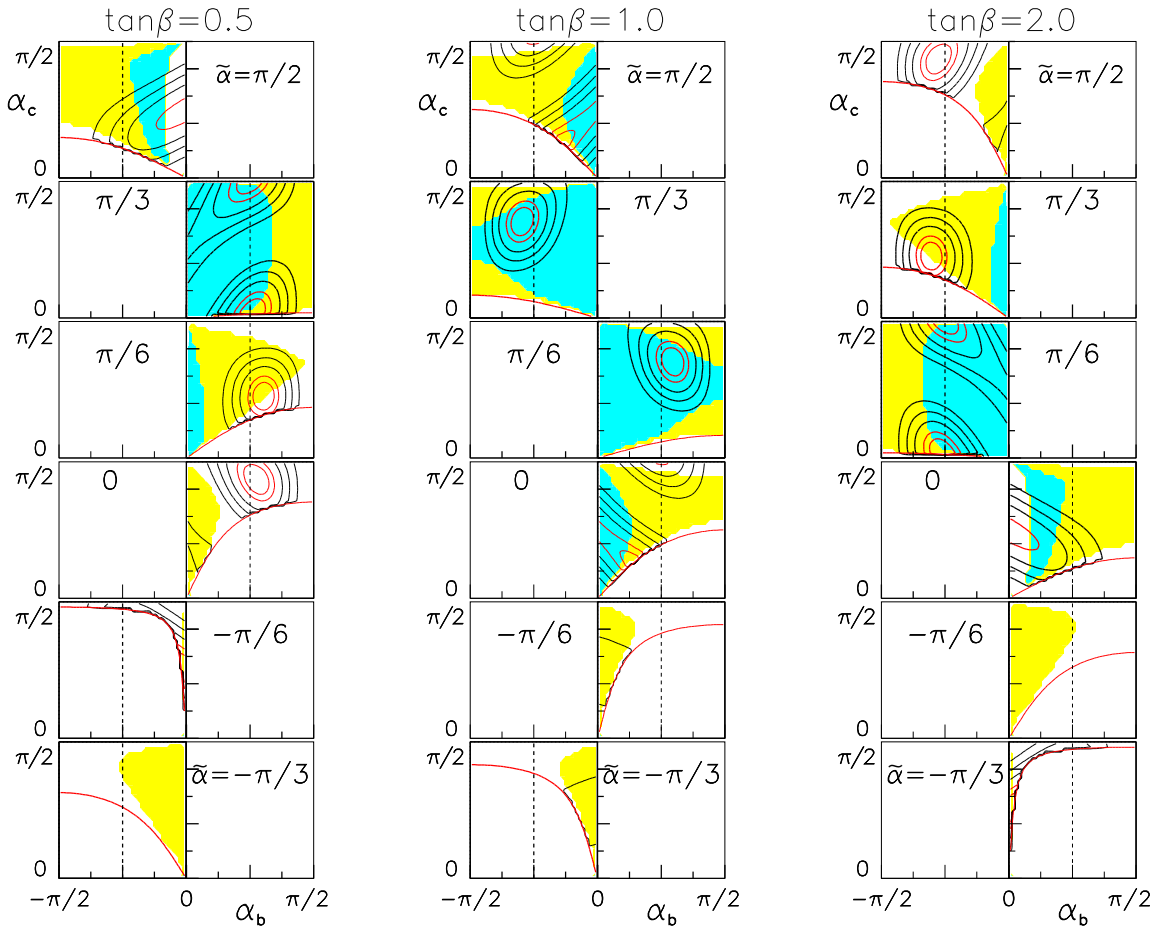

Figure 2: Contours of constant ξ_V [see Eq. (3.1)] in the α_b–α_c plane for various values of $\tan\beta$ and $\tilde{\alpha}$. Soft parameters: $M_1 = 100$ GeV, $M_2 = 500$ GeV, $M_{H^\pm} = 600$ GeV, $\mu = 300$ GeV. Dark (blue): $\xi_{\rm pert} = 1$, light (yellow): $\xi_{\rm pert} = 5$.

$\alpha_b = 0$

For $\alpha_b = 0$, the rotation matrix simplifies:

$$R = \begin{pmatrix} c_{\tilde{\alpha}} & s_{\tilde{\alpha}} & 0 \\ -s_{\tilde{\alpha}}\, c_c & c_{\tilde{\alpha}}\, c_c & s_c \\ s_{\tilde{\alpha}}\, s_c & -c_{\tilde{\alpha}}\, s_c & c_c \end{pmatrix}, \tag{3.4}$$

and one finds

$$\xi_V(\alpha_b = 0) = \frac{27}{4}\, \sin^2(2\alpha_c)\, \sin^4(\beta - \tilde{\alpha})\, \cos^2(\beta - \tilde{\alpha}). \tag{3.5}$$

The maximum is given by

$$\xi_V = 1 \quad \text{for} \quad \tilde{\alpha} = \beta \pm \arctan\sqrt{2}, \quad \alpha_b = 0, \quad \alpha_c = \pm\pi/4. \tag{3.6}$$

$\alpha_c = 0$

For $\alpha_c = 0$, one finds

$$\xi_V(\alpha_c = 0) = \frac{27}{4} \sin^2(2\alpha_b) \cos^4(\beta - \tilde{\alpha}) \sin^2(\beta - \tilde{\alpha}). \tag{3.7}$$

This relation holds also for $\alpha_c = \pi/2$. The maximum is given by

$$\xi_V = 1 \quad \text{for} \quad \tilde{\alpha} = \beta \pm \arctan(1/\sqrt{2}), \quad \alpha_b = \pm\pi/4, \quad \alpha_c = 0 \text{ or } \alpha_c = \pi/2. \tag{3.8}$$

3.2 Maxima of ξ_V

Since maximizing over angles allows us to keep *two* Higgs masses fixed [5] and since by Eq. (3.2), the dependence of ξ_V on β and $\tilde{\alpha}$ shows up in the form $(\beta - \tilde{\alpha})$, ξ_V can be maximized for fixed $(\beta - \tilde{\alpha})$ by meeting the two conditions:

$$\frac{\partial \xi_V}{\partial \alpha_b} = 0 \qquad \text{and} \qquad \frac{\partial \xi_V}{\partial \alpha_c} = 0. \tag{3.9}$$

By substituting from Eq. (3.2), and solving (3.9) for α_b and α_c, we obtain a continuum of maxima:

$$\begin{aligned} \xi_V = 1 \quad \text{for} \quad & \alpha_b = \pm \arccos \sqrt{\frac{1 + \tan^2(\beta - \tilde{\alpha})}{3}}, \\ & \alpha_c = \pm \arctan \frac{1 + \tan^2(\beta - \tilde{\alpha}) - \sqrt{3[2 - \tan^2(\beta - \tilde{\alpha})]}\, \tan(\beta - \tilde{\alpha})}{2\tan^2(\beta - \tilde{\alpha}) - 1}. \end{aligned} \tag{3.10}$$

which impose the constraint

$$|\tan(\beta - \tilde{\alpha})| \leq \sqrt{2} \tag{3.11}$$

on $(\beta - \tilde{\alpha})$. We note that (3.6) and (3.8) are both special cases of this (3.10).

We show in Fig. 3 how these angles α_b and α_c vary with $\tan\beta$ (for fixed $\tilde{\alpha}$) when we maximize ξ_V. For a given value of $\tilde{\alpha}$, these curves only cover a finite range in $\tan\beta$. They are cut off by (3.11), which says that, in order to have $\xi_V = 1$, β and $\tilde{\alpha}$ should not differ by more than $\arctan\sqrt{2} \simeq 54.7\,^\circ$. In addition, they are cut off by the condition of having a physical solution as discussed in sect. 2, and delineated by the solid contours in Fig. 1. Note that there are also solutions having other signs for α_b and α_c, but that the model is only physically consistent for certain sign combinations.

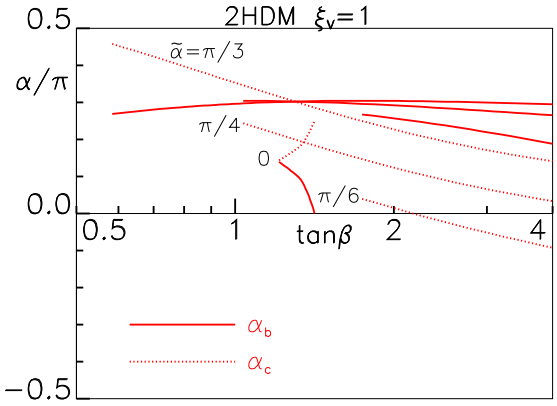

Figure 3: Angles α_b and α_c [cf. Eq. (3.10)] for which the CP nonconservation ξ_V in the gauge-Higgs sector is maximal, for a range of $\tan\beta$ values, and for $\tilde{\alpha} = 0$, $\pi/6$, $\pi/4$, and $\pi/3$.

4 CP nonconservation in the Yukawa sector

In the Yukawa sector, one can define measures of CP nonconservation analogous to the one for the gauge-Higgs sector [cf. ξ_V of Eq. (1.1)]. Requiring thus that *all three* Higgs bosons should have CP-nonconserving couplings to up- and down-type quarks, it is natural to consider the quantities [see Eqs. (2.8), (2.9) and (5.3)]:

$$\begin{aligned} \xi_t &= \left(\frac{\cos\beta}{\sin^2\beta}\right)^6 \prod_{i=1}^{3} [R_{i2}\, R_{i3}]^2 \equiv \left(\frac{\cos\beta}{\sin^2\beta}\right)^6 \tilde{\gamma}_t, \\ \xi_b &= \left(\frac{\sin\beta}{\cos^2\beta}\right)^6 \prod_{i=1}^{3} [R_{i1}\, R_{i3}]^2 \equiv \left(\frac{\sin\beta}{\cos^2\beta}\right)^6 \tilde{\gamma}_b. \end{aligned} \tag{4.1}$$

Both of these differ from the ξ_V defined above in two respects. First of all, the dependence on β factorizes. Secondly, they individually diverge as $\sin\beta \to 0$ (for up-type quarks) or $\cos\beta \to 0$ (for down-type quarks).

One could also consider the quantities

$$\zeta_t = \left(\frac{\cos\beta}{\sin^2\beta}\right)^2 \sum_{i=1}^{3} [R_{i2}\, R_{i3}]^2 \tag{4.2}$$

and similarly ζ_b as measures of CP nonconservation in the Yukawa sector. These measures—unlike those in (4.1)—are consistent with the fact that if H_1 conserves CP in its couplings

to the up- and down-type quarks, i.e. $\alpha_b = 0$, then the Yukawa sector *may still be CP nonconserving*, since the other two Higgs states, H_2 and H_3, may have CP nonconserving couplings to the quarks. Accordingly, $\zeta_t \neq 0$ and $\zeta_b \neq 0$ for $\alpha_b = 0$ which is not the case for ξ_t and ξ_b. This ζ_t will be discussed in sect. 4.3.

Substituting now from (2.4) into (4.1), we obtain for this case of Model II Yukawa couplings:

$$\tilde{\gamma}_t = c_b^6 (s_{\tilde{\alpha}}\, s_b\, c_c\, s_c)^2 [s_{\tilde{\alpha}}\, s_b\, c_c + c_{\tilde{\alpha}}\, s_c]^2 [s_{\tilde{\alpha}}\, s_b\, s_c - c_{\tilde{\alpha}}\, c_c]^2,$$
$$\tilde{\gamma}_b = c_b^6 (c_{\tilde{\alpha}}\, s_b\, c_c\, s_c)^2 [c_{\tilde{\alpha}}\, s_b\, s_c + s_{\tilde{\alpha}}\, c_c]^2 [c_{\tilde{\alpha}}\, s_b\, c_c - s_{\tilde{\alpha}}\, s_c]^2. \tag{4.3}$$

We note that both these quantities possess the same symmetries (3.3) as ξ_V. Also, $\tilde{\gamma}_b$ is obtained from $\tilde{\gamma}_t$ by the substitutions

$$(s_{\tilde{\alpha}} \leftrightarrow c_{\tilde{\alpha}}), \quad (s_c \leftrightarrow c_c): \qquad \tilde{\gamma}_t \leftrightarrow \tilde{\gamma}_b. \tag{4.4}$$

4.1 Maxima of γ_t

Let us now consider the maxima of $\tilde{\gamma}_t$ in (4.3). We find the maximum value $\tilde{\gamma}_t^{\max} = 1/1024$ for

$$\text{Case I}: \quad \tilde{\alpha} = \tfrac{1}{2}\pi, \quad \alpha_b = \pm\tfrac{1}{4}\pi, \quad \alpha_c = \pm\tfrac{1}{4}\pi, \tag{4.5}$$

where the two signs are independent, and at

$$\text{Case II}: \quad \tilde{\alpha} = \pm \arctan\frac{1}{\sqrt{2}}\ (\tilde{\alpha} = \pm 0.196\,\pi), \quad \alpha_b = \pm\tfrac{1}{6}\pi, \quad \text{with}$$
$$\alpha_c = \pm \arctan\frac{1}{\sqrt{2}}\ (\alpha_c = \pm 0.196\,\pi) \quad \text{or} \quad \alpha_c = \mp \arctan\sqrt{2}\ (\alpha_c = \pm 0.304\,\pi). \tag{4.6}$$

For Case II, the signs are subject to the constraint $\tilde{\alpha}\alpha_b\alpha_c > 0$ for the first α_c solution, and $\tilde{\alpha}\alpha_b\alpha_c < 0$ for the second α_c solution. The maxima of $\tilde{\gamma}_b$ are obtained by the substitutions (4.4).

Thus, it is natural to define normalized quantities

$$\gamma_t = 1024 \prod_{i=1}^{3} [R_{i2}\, R_{i3}]^2, \quad \gamma_b = 1024 \prod_{i=1}^{3} [R_{i1}\, R_{i3}]^2, \tag{4.7}$$

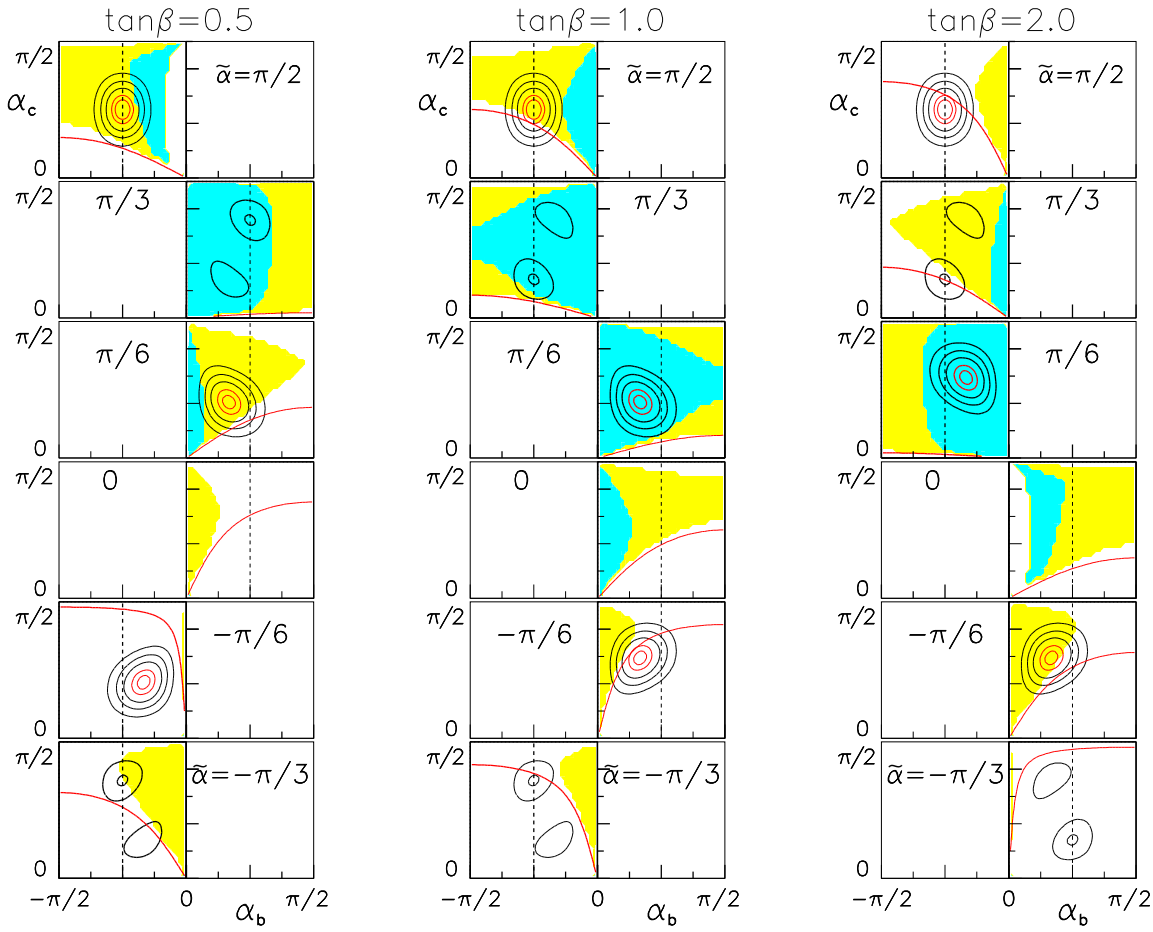

Figure 4: Contours of constant γ_t [see Eq. (4.7)] in the α_b–α_c plane for various values of $\tan\beta$ and $\tilde{\alpha}$. Soft parameters: $M_1 = 100$ GeV, $M_2 = 500$ GeV, $M_{H^\pm} = 600$ GeV, $\mu = 300$ GeV. Dark (blue): $\xi_{\rm pert} = 1$, light (yellow): $\xi_{\rm pert} = 5$.

satisfying

$$0 \le \gamma_t \le 1, \quad 0 \le \gamma_b \le 1, \tag{4.8}$$

as measures of CP nonconservation in the up- and down-quark sectors, respectively. Contours of constant γ_t are shown in the α_b–α_c-plane in Fig. 4.

Let us now keep $\tilde{\alpha}$ fixed. Then, the maxima of γ_t are at

$$\begin{aligned} &\text{Case I}: \quad \alpha_b = \epsilon_b \tfrac{1}{4}\pi, \quad \alpha_c = \epsilon_c \arctan\Big[\sqrt{2}\Big(\sqrt{\tan^{-2}\tilde{\alpha} + \tfrac{1}{2}} + \epsilon_b\,\epsilon_c\,\tan^{-1}\tilde{\alpha}\Big)\Big], \\ &\text{Case II}: \quad \alpha_b = \epsilon_b \tfrac{1}{6}\pi, \quad \alpha_c = \epsilon_c \arctan\Big[\tfrac{1}{2}\Big(\sqrt{\tan^{2}\tilde{\alpha} + 4} - \epsilon_b\,\epsilon_c\,\tan\tilde{\alpha}\Big)\Big], \end{aligned} \tag{4.9}$$

where ϵ_b and ϵ_c are independent sign factors: $\epsilon_b = \pm 1$, $\epsilon_c = \pm 1$. For Case I, the corre-

sponding maximum is (same for all sign choices)

$$\gamma_t = \sin^6 \tilde{\alpha}, \tag{4.10}$$

in agreement with Eq. (4.5), whereas for Case II, the corresponding maximum is (same for all sign choices)

$$\gamma_t = \frac{27}{4} \frac{\tan^2 \tilde{\alpha}}{(1+\tan^2 \tilde{\alpha})^3}, \tag{4.11}$$

which becomes 1 for $\tan \tilde{\alpha} = \pm 1/\sqrt{2}$, in agreement with Eq. (4.6).

4.2 Maxima of ξ_Y

While ξ_t and ξ_b individually diverge as $\beta \to 0$ and $\beta \to \pi/2$, respectively, the product over couplings to up-type and down-type quarks is less divergent. We define, analogous to (1.1) and (4.1)

$$\xi_Y \equiv \xi_t \, \xi_b \equiv \frac{1}{(\cos\beta \sin\beta)^6} \, \gamma_Y, \tag{4.12}$$

with

$$\gamma_Y = \gamma_0 \, \tilde{\gamma}_t \, \tilde{\gamma}_b = \gamma_0 \prod_{i=1}^{3} \left[R_{i1} \, R_{i2} \, R_{i3}^2 \right]^2 . \tag{4.13}$$

satisfying

$$0 \le \gamma_Y \le 1. \tag{4.14}$$

Substituting from (4.3), we obtain

$$\begin{aligned} \gamma_Y = \gamma_0 \, c_b^{12} (c_c \, s_c \, s_b)^4 (c_{\tilde{\alpha}} \, s_{\tilde{\alpha}})^2 [s_{\tilde{\alpha}} \, c_c \, s_b + c_{\tilde{\alpha}} \, s_c]^2 [c_{\tilde{\alpha}} \, c_c \, s_b - s_{\tilde{\alpha}} \, s_c]^2 \\ \times [c_{\tilde{\alpha}} \, s_b \, s_c + s_{\tilde{\alpha}} \, c_c]^2 [s_{\tilde{\alpha}} \, s_b \, s_c - c_{\tilde{\alpha}} \, c_c]^2 . \end{aligned} \tag{4.15}$$

This has a maximum for (see Appendix A)

$$\tilde{\alpha} = \pm \tfrac{1}{4}\pi, \qquad \alpha_b = \pm \arcsin \sqrt{\tfrac{1}{6}} = \pm 0.13386\pi \quad (24.1\,^\circ), \qquad \alpha_c = \pm \tfrac{1}{4}\pi, \tag{4.16}$$

with

$$\gamma_0 = \frac{2^{26} \, 3^{12}}{5^{10}} = \left(\frac{8 \times 1024 \times 27^2}{3125} \right)^2 = 3.652 \times 10^6. \tag{4.17}$$

Fig. 5 exhibits contours of constant γ_Y for some values of $\tilde{\alpha}$ other than that of the maximum, $\tilde{\alpha} = \frac{1}{4}\pi$, in relation to the physically allowed (dark, shaded) regions in the

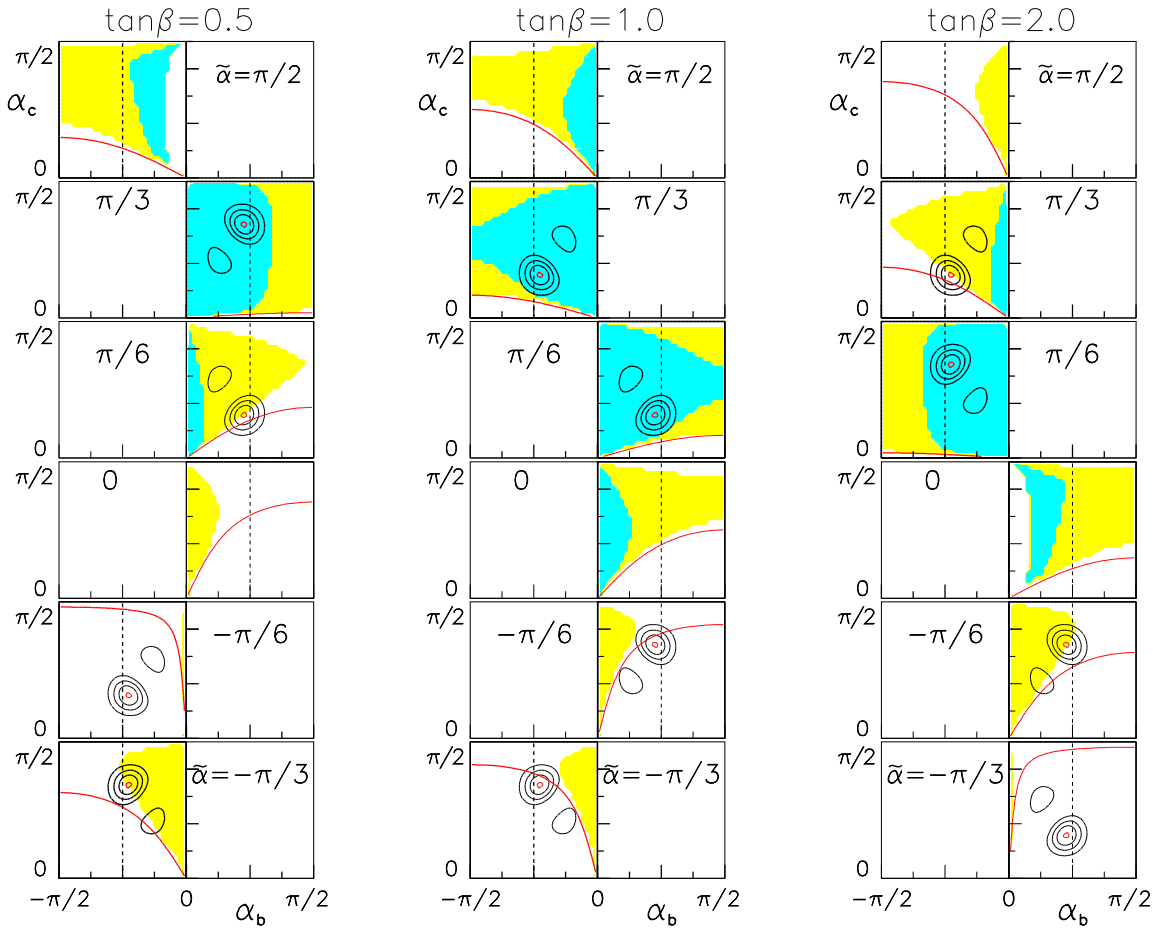

Figure 5: Contours of constant γ_Y in the α_b–α_c plane for various values of $\tan\beta$ and $\tilde{\alpha}$. Soft parameters: $M_1 = 100$ GeV, $M_2 = 500$ GeV, $M_{H^\pm} = 600$ GeV, $\mu = 300$ GeV. Dark (blue): $\xi_{\rm pert} = 1$, light (yellow): $\xi_{\rm pert} = 5$.

α_b–α_c plane. Note that γ_Y vanishes when $\tilde{\alpha} = 0$ or $\tilde{\alpha} = \pm\pi/2$, as well as on the edges of the quadrants: $\alpha_b = 0$ or $\pm\pi/2$, $\alpha_c = 0$ or $\pm\pi/2$. Also, we note that there are secondary, local, maxima.

Although γ_Y is, by definition, independent of β, Fig. 5 shows contours of constant γ_Y superimposed on allowed regions for different values of $\tan\beta$, since the 'shapes' and locations of the physically allowed regions in the α_b–α_c plane depend on $\tan\beta$. Accordingly, the positions of the maxima[2] of γ_Y, w.r.t. the physically allowed regions in the α_b–α_c plane are different for different values of $\tan\beta$. For example, consider $\tilde{\alpha} = \pi/6$. We see from

[2]This is not a 'maximum' in the same sense as above, since $\tilde{\alpha}$ is held fixed.

Fig. 5 that for $\tan\beta = 0.5$, $\gamma_Y^{\max}$ is located *outside* the physically allowed region while for $\tan\beta = 1.0$, this is not the case. Moreover, for $\tan\beta = 2.0$, the physically allowed region shifts the location to the 'other' quadrant. To sum up, for $\tilde{\alpha} = \pi/6$, the location of $\gamma_Y^{\max}$ occurs at

$$(\alpha_b, \alpha_c)|_{\tan\beta=0.5} = (\alpha_b, \alpha_c)|_{\tan\beta=1.0} = (-\alpha_b, \pi/2 - \alpha_c)|_{\tan\beta=2.0}.$$

4.3 Maximizing ζ_t

We now return to the quantity ζ_t of Eq. (4.2), which we rewrite as

$$\zeta_t = \left(\cos\beta/\sin^2\beta\right)^2 \tilde{\zeta}_t \tag{4.18}$$

with

$$\tilde{\zeta}_t = 2\sum_{i=1}^{3}[R_{i2}\,R_{i3}]^2, \quad 0 < \tilde{\zeta}_t < 1. \tag{4.19}$$

Substituting from (2.4) and utilising trigonometric identities, we find

$$\tilde{\zeta}_t = \tfrac{1}{4}c_b^2[(1 - c_{2\tilde{\alpha}})(7 + c_{4c})s_b^2 + 2s_{2\tilde{\alpha}}s_{4c}s_b + (1 + c_{2\tilde{\alpha}})(1 - c_{4c})]. \tag{4.20}$$

To maximize $\tilde{\zeta}_t$, we differentiate w.r.t. $\tilde{\alpha}$, α_b and α_c and get:

$$\begin{aligned} s_{2\tilde{\alpha}}(7 + c_{4c})s_b^2 + 2c_{2\tilde{\alpha}}s_{4c}s_b - s_{2\tilde{\alpha}}(1 - c_{4c}) = 0, \\ 2(1 - c_{2\tilde{\alpha}})(7 + c_{4c})s_b^3 + 3s_{2\tilde{\alpha}}s_{4c}s_b^2 - 2(3 - 4c_{2\tilde{\alpha}} + c_{4c})s_b - s_{2\tilde{\alpha}}s_{4c} = 0, \\ (1 - c_{2\tilde{\alpha}})s_{4c}s_b^2 - 2s_{2\tilde{\alpha}}c_{4c}s_b - (1 + c_{2\tilde{\alpha}})s_{4c} = 0. \end{aligned} \tag{4.21}$$

Solving the three equations, one finds: $\tilde{\zeta}_t = 1$ for

$$\begin{aligned} \text{Case I}: &\quad c_{2\tilde{\alpha}} = 1, \quad s_b = 0, \quad c_{4c} = -1 \\ \text{Case II}: &\quad c_{2\tilde{\alpha}} = -1, \quad s_b = \pm 1/\sqrt{2}, \quad c_{4c} = 1 \end{aligned} \tag{4.22}$$

with the corresponding angles

$$\begin{aligned} \text{Case I}: &\quad \tilde{\alpha} = 0, \quad \alpha_b = 0 \text{ or } \alpha_b = \pm\pi, \quad \alpha_c = \pm\tfrac{1}{4}\pi, \\ \text{Case II}: &\quad \tilde{\alpha} = \pm\tfrac{1}{2}\pi, \quad \alpha_b = \pm\tfrac{1}{4}\pi, \quad \alpha_c = 0 \text{ or } \pm\tfrac{1}{2}\pi. \end{aligned} \tag{4.23}$$

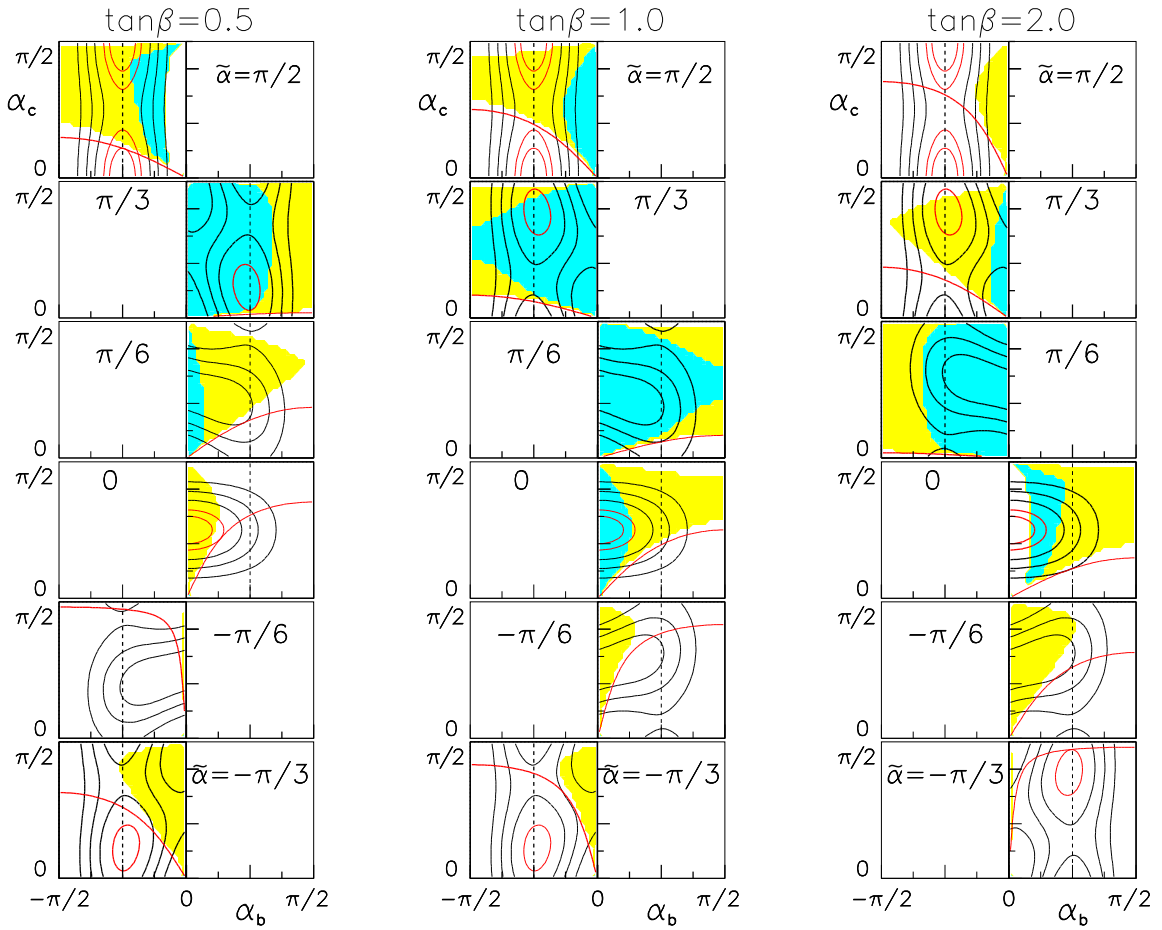

Figure 6: Contours of constant $\tilde{\zeta}_t$ [see Eq. (4.20)] in the α_b–α_c plane for various values of $\tan\beta$ and $\tilde{\alpha}$. Soft parameters: $M_1 = 100$ GeV, $M_2 = 500$ GeV, $M_{H^\pm} = 600$ GeV, $\mu = 300$ GeV. Dark (blue): $\xi_{\rm pert} = 1$, light (yellow): $\xi_{\rm pert} = 5$.

Considering now $\tilde{\alpha}$ fixed, we find the maxima:

$$\text{Case I}: \quad \alpha_b = 0 \text{ (or } \pm\pi), \quad \alpha_c = \pm\tfrac{1}{4}\pi, \tag{4.24}$$

for which

$$\tilde{\zeta}_t = \tfrac{1}{2}(1 + c_{2\tilde{\alpha}}) \tag{4.25}$$

coincides with Case I in (4.22) for $c_{2\tilde{\alpha}} = 1$, and

$$\text{Case II}: \quad \alpha_b = \pm\arcsin\frac{\sqrt{3-5c_{2\tilde{\alpha}}}}{2\sqrt{2}\sqrt{1-c_{2\tilde{\alpha}}}}, \quad \alpha_c = \pm\frac{1}{4}\left[\pi - \arccos\frac{5+13c_{2\tilde{\alpha}}}{11+3c_{2\tilde{\alpha}}}\right], \tag{4.26}$$

provided $c_{2\tilde{\alpha}} \leq 3/5$. In this case

$$\tilde{\zeta}_t = \frac{(5-3c_{2\tilde{\alpha}})}{32(1-c_{2\tilde{\alpha}})(11+3c_{2\tilde{\alpha}})^2}\big[(11+3c_{2\tilde{\alpha}})(43-10c_{2\tilde{\alpha}}+11c_{2\tilde{\alpha}}^2) + (44+12c_{2\tilde{\alpha}})\sqrt{3-5c_{2\tilde{\alpha}}}\sqrt{1+c_{2\tilde{\alpha}}}\sqrt{3-2c_{2\tilde{\alpha}}-5c_{2\tilde{\alpha}}^2}\big], \tag{4.27}$$

agrees with Case II in (4.22) for $c_{2\tilde{\alpha}} = -1$.

Fig. 6 exhibits contours of constant $\tilde{\zeta}_t$ in the α_b–α_c plane for selected values of $\tan\beta$ and $\tilde{\alpha}$. We read off from Fig. 6 that for $\tilde{\alpha} = 0$, the quantity $\tilde{\zeta}_t$ takes its maximum value at $(\alpha_b, \alpha_c) = (0, \frac{1}{4}\pi)$ which again is consistent with Case I in (4.22). For particular values of $\tilde{\alpha}$ and α_c, there are also saddle points, for example at $(\tilde{\alpha}, \alpha_b, \alpha_c) = (\frac{1}{2}\pi, -\frac{1}{4}\pi, \frac{1}{4}\pi)$. For a given value of $\tilde{\alpha}$, these saddle points are located at

$$\alpha_b = \pm\tfrac{1}{4}\pi, \quad \alpha_c = \pm\tfrac{1}{4}\arccos\left(\frac{1+3c_{2\tilde{\alpha}}}{3+c_{2\tilde{\alpha}}}\right) \tag{4.28}$$

in the α_b–α_c plane.

In the top-Higgs Yukawa sector, γ_t [see Eq. (4.7)] and $\tilde{\zeta}_t$ are both sizable for large $\tilde{\alpha}$ and $|\alpha_b| \simeq \pi/4$, as we see in Figs. 4 and 6. However, the two measures have different features. For example, for the same value of $\tilde{\alpha} = 0$, where $\tilde{\zeta}_t$ has a maximum, γ_t vanishes. Moreover, for $\alpha_b = 0$, γ_t vanishes (regardless the values of $\tilde{\alpha}$ and α_c) while $\tilde{\zeta}_t$ takes its maximum value (for $\tilde{\alpha} = 0$ and $\alpha_c = \frac{1}{4}\pi$). This again shows that these quantities γ_t and $\tilde{\zeta}_t$ behave rather differently for a given set of the angles $(\tilde{\alpha}, \alpha_b, \alpha_c)$.

5 CP nonconservation in $pp \to t\bar{t}$

The above studies refer to the tree-level couplings of Higgs particles to vector particles and fermions. These are difficult to study directly, since the Higgs particles as well as the vector particles and the relevant fermions are unstable. The implication is that it is easier to access these couplings via various loop effects. We shall here consider one such example, namely the production amplitudes for the $t\bar{t}$ through gluon fusion, where CP nonconservation is induced by non-standard neutral Higgs exchange.

CP nonconservation in the production of $t\bar{t}$ pairs at future hadronic colliders has been studied in considerable detail [7]. For a detailed application to the 2HDM, see also [5].

One process of particular interest is

$$pp \to t\bar{t}X, \tag{5.1}$$

where the t and $\bar{t}$ decay semileptonically, and the lepton energy difference is measured [5,7]:

$$A_1 = E_+ - E_-. \tag{5.2}$$

(For a discussion of other observables, see [7,8].) The expectation value of this observable will in general be non-zero if there between the quarks in the final state are exchanges of Higgs bosons that are not eigenstates under CP. The quantity [see Eq. (2.8)]

$$\gamma_{CP,j} = -a_j^{(t)} \tilde{a}_j^{(t)} = \frac{\cos\beta}{\sin^2\beta} R_{j2} R_{j3} \tag{5.3}$$

then plays a crucial role, together with non-trivial functions of the kinematics (given by the loop integrals).

If the neutral-Higgs spectrum has a large gap between the lightest Higgs boson and the next one, then the lightest one will give the dominant contribution to A_1, and the amount of CP nonconservation is roughly proportional to

$$\gamma_{CP,1} = \tfrac{1}{2} \frac{\sin\tilde{\alpha}\sin(2\alpha_b)}{\tan\beta\sin\beta}, \tag{5.4}$$

which is maximized for small $\tan\beta$ and for $(\tilde{\alpha}, \alpha_b) = (\pm\pi/2, \pm\pi/4)$, corresponding to the dashed lines at $\alpha_b = \pm\pi/4$ in Figs. 1, 2, 4, 5 and 6. These values as well, $(\tilde{\alpha}, \alpha_b) = (\pm\pi/2, \pm\pi/4)$, together with $\alpha_c = 0$ or $\pm\frac{1}{2}\pi$, coincide with those of Case II [see Eq. (4.23)] that maximize $\tilde{\zeta}_t$. Furthermore, $(\tilde{\alpha}, \alpha_b) = (\pi/2, \pm\pi/4)$, together with $\alpha_c = \pm\frac{1}{4}\pi$, coincide with those of Case I [see Eq. (4.5)] that maximize γ_t. These results indicate that large $\tilde{\alpha}$ together with $|\alpha_b| \simeq \pi/4$ favour large CP nonconservation in the Yukawa sector. It is immediately obvious that this is not compatible with the condition of maximal CP nonconservation in the gauge–Higgs sector [1], $\xi_V = 1$ [see Eqs. (3.6) and (3.8)].

In addition to the contribution from the lightest Higgs boson, there will in general also be non-negligible contributions from the others. Because of the orthogonality of the rotation matrix R, not all $\gamma_{CP,j}$ can have the same sign, so there will be cancellations.

Let us define the 'signal-to-noise ratio', or sensitivity [7]

$$\frac{S}{N} = \frac{\langle A_1 \rangle}{\sqrt{\langle A_1^2 \rangle - \langle A_1 \rangle^2}}, \tag{5.5}$$

which provides a measure of how much data would be required to see an effect.

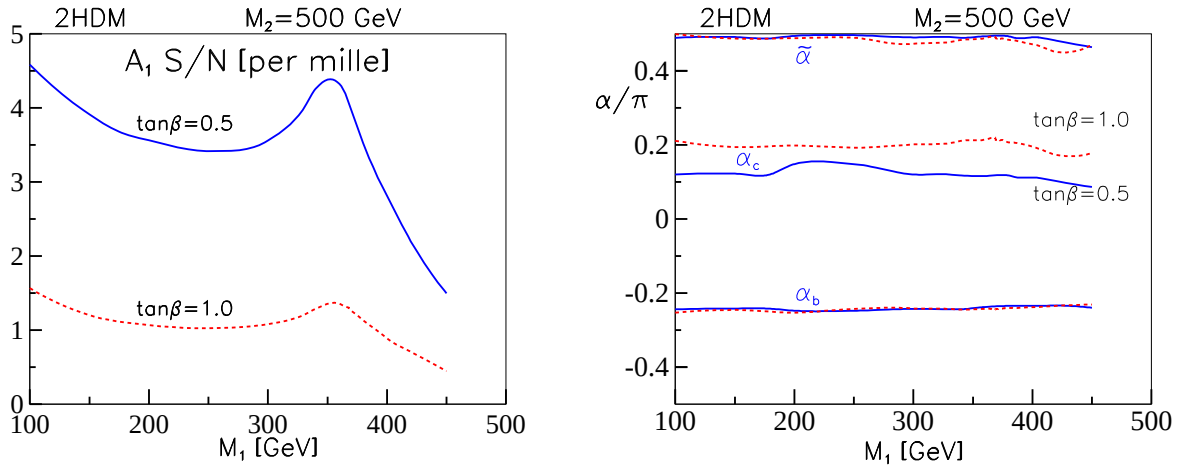

Figure 7: Left panel: Maximal sensitivity [see (5.5)] for the observable (5.2), for fixed M_1, M_2 and two values of $\tan\beta$. Right panel: Corresponding values of the angles $\tilde{\alpha}$, α_b and α_c. Soft parameters: $M_2 = 500$ GeV, $M_{H^\pm} = 600$ GeV, $\xi_{\rm pert} = 5$.

It is interesting to maximize the amount of CP nonconservation that results for the observable A_1, over the relevant parameters of the model. In Fig. 7 we show the result of such a maximization of the sensitivity (5.5). The quantity A_1 and its spread A_1^2 are computed as given in [5, 7], using the 'LoopTools' package [9, 10], and convoluted with the CTEQ6 parton distribution functions [11] for the LHC energy of 14 TeV. The resulting quantity is then maximized using the 'MINUIT' package [12].

The actual maximization is rather CPU-intensive: In order to evaluate A_1 and S/N, three-dimensional integrals (a convolution integral over the parton distribution functions, an integral over the polar angle of the top quark with respect to the beam, an integral over $\hat{s}$, the invariant mass squared of the $t\bar{t}$ pair) involving non-trivial loop functions are required. These are then maximized in the three angles parameterizing the 2HDM mass matrix: $\tilde{\alpha}$, α_b and α_c (keeping the two lowest Higgs masses fixed).

In this maximization, we have kept $M_2 = 500$ GeV fixed, and considered two values of $\tan\beta$ (0.5 and 1.0), and a range of values of M_1. The resulting angles $\tilde{\alpha}$ and α_b are rather independent of M_1 as well as the choice of $\tan\beta$, whereas α_c has some dependence on $\tan\beta$, as shown in the right panel of Fig. 7.

For a given value of M_1, the resulting maximum is close to that found in [5], maximizing only with respect to the H_1 contribution. We note that, considered as a function of M_1, there is a peak associated with the $t\bar{t}$ threshold. This is due to the contribution of the $t\bar{t}$ triangle diagram [5, 7].

As discussed in [5], the heavier Higgs states have a tendency to reduce the CP-violating effect of the lightest one, unless they are sufficiently heavy to decouple. Thus, for a fixed value of the lightest Higgs mass, M_1, the over-all CP-nonconservation should increase as the second Higgs boson becomes heavier. This effect is illustrated in Fig. 8 for the case of $M_1 = 100$ GeV and two values of $\tan\beta$ (0.5 and 1.0). Apart from some wiggles due to numerical noise, it is seen that there is a rather smooth increase of the sensitivity as the mass gap $M_2 - M_1$ increases.

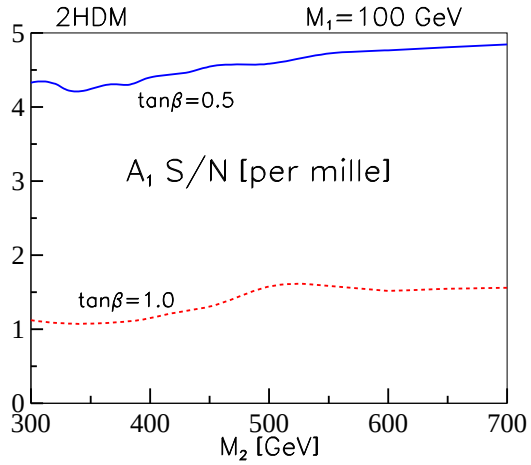

Figure 8: Maximum sensitivity S/N [see (5.5)] *vs.* M_2, for fixed $M_1 = 100$ GeV. Soft parameters: $M_{H^\pm} = 700$ GeV, $\xi_{\rm pert} = 5$.

Let us now comment on the maximum CP nonconservation in the Yukawa sector, as given by the sensitivity in the quantity A_1, compared with that of the gauge-Higgs sector,

ξ_V. We already stated that these concepts are different. This statement can be made quantitative by considering the value of ξ_V that corresponds to the rotation angles $\tilde{\alpha}$, α_b and α_c for which the sensitivity in A_1 is maximal. We find that $\xi_V \simeq 0.6$ and 0.3, for $\tan\beta = 0.5$ and 1.0, respectively.

6 Concluding remarks

The concept of maximal CP nonconservation has been extended from the gauge–Higgs sector to the Yukawa sector, where various measures for CP nonconservation have been introduced and investigated. Large values of $\tilde{\alpha}$ and $|\alpha_b| \simeq \pi/4$ favour large CP nonconservation in the Yukawa sector. But, in general, the maxima of CP nonconservation will in these two sectors not coincide. There could even be *maximal* CP nonconservation in one sector, and little or none in the other.

We have here studied the *simplest* version of the 2HDM that allows for CP nonconservation, where this CP nonconservation is given by *one* parameter, namely $\mathrm{Im}\,\lambda_5$ in the potential (2.1). One could consider two more, independent parameters in the Higgs potential that generate CP nonconservation, namely $\mathrm{Im}\,\lambda_6$ and $\mathrm{Im}\,\lambda_7$ (see, e.g., [6]). These terms in the potential are often considered less attractive, since they violate the Z_2 symmetry of the potential by terms which are quartic in the Higgs fields and thus make it more difficult to control flavour-changing neutral currents [13, 14].

However, if present, such terms would lead to a less constrained theory. While the Yukawa couplings (for Model II) are still given by the same elements of the rotation matrix R (and hence by the same expression in terms of $\tan\beta$ and the rotation angles $\tilde{\alpha}$, α_b and α_c), the masses M_2 and M_3 would be less constrained. By making these masses larger, the contribution of the lightest one, H_1, would be a better approximation to the over-all CP nonconservation.

Acknowledgments: It is a pleasure to thank the organizers of the Epiphany 2003 Conference for creating a most stimulating atmosphere, and for excellent hospitality.

Appendix A. Maximizing γ_Y

This appendix deals with the maximization of γ_Y, Eq. (4.13). We shall first rewrite $\tilde{\gamma}_b\tilde{\gamma}_t$ in terms of double angles. Let

$$\begin{aligned} x &\equiv (s_{\tilde{\alpha}}\, s_b\, c_c + c_{\tilde{\alpha}}\, s_c)(c_{\tilde{\alpha}}\, s_b\, c_c - s_{\tilde{\alpha}}\, s_c), \\ y &\equiv (c_{\tilde{\alpha}}\, s_b\, s_c + s_{\tilde{\alpha}}\, c_c)(s_{\tilde{\alpha}}\, s_b\, s_c - c_{\tilde{\alpha}}\, c_c), \end{aligned} \tag{A.1}$$

then

$$\tilde{\gamma}_b\tilde{\gamma}_t = z^2 \tag{A.2}$$

with

$$z = c_b^6\, c_{\tilde{\alpha}}\, s_{\tilde{\alpha}}\, s_b^2 (c_c s_c)^2\, xy. \tag{A.3}$$

Maximizing $\tilde{\gamma}_b\tilde{\gamma}_t$ amounts to maximizing the absolute value of z.

We first note that

$$x = \tfrac{1}{4} s_{2\tilde{\alpha}}[(1+s_b^2)c_{2c} - c_b^2] + \tfrac{1}{2} c_{2\tilde{\alpha}}\, s_b\, s_{2c} \tag{A.4}$$

where $c_{2\tilde{\alpha}} = \cos(2\tilde{\alpha})$, $c_{2c} = \cos(2\alpha_c)$, etc. Furthermore, y can be obtained from x by the substitutions $c_{\tilde{\alpha}} \leftrightarrow s_{\tilde{\alpha}}$ and $c_c \leftrightarrow s_c$, implying $c_{2\tilde{\alpha}} \leftrightarrow -c_{2\tilde{\alpha}}$, $c_{2c} \leftrightarrow -c_{2c}$, with $s_{2\tilde{\alpha}}$ and s_{2c} unchanged. Thus,

$$\begin{aligned} xy &= \{-\tfrac{1}{4} s_{2\tilde{\alpha}}\, c_b^2 + [\tfrac{1}{2} c_{2\tilde{\alpha}}\, s_b\, s_{2c} + \tfrac{1}{4} s_{2\tilde{\alpha}}(1+s_b^2)c_{2c}]\} \\ &\quad \times \{-\tfrac{1}{4} s_{2\tilde{\alpha}}\, c_b^2 - [\tfrac{1}{2} c_{2\tilde{\alpha}}\, s_b\, s_{2c} + \tfrac{1}{4} s_{2\tilde{\alpha}}(1+s_b^2)c_{2c}]\} \\ &= \tfrac{1}{16}[s_{2\tilde{\alpha}}^2\, c_b^4 - 4c_{2\tilde{\alpha}}^2\, s_b^2\, s_{2c}^2 - s_{2\tilde{\alpha}}^2(1+s_b^2)^2 c_{2c}^2 - 4c_{2\tilde{\alpha}}\, s_{2\tilde{\alpha}}(1+s_b^2)\, s_b\, c_{2c}\, s_{2c}] \end{aligned} \tag{A.5}$$

The maximum is given by the three conditions:

$$\frac{\partial z}{\partial \tilde{\alpha}} = 0, \qquad \frac{\partial z}{\partial \alpha_b} = 0, \qquad \frac{\partial z}{\partial \alpha_c} = 0, \tag{A.6}$$

or equivalently:

$$\begin{aligned} &3c_{2\tilde{\alpha}}\,(1-c_{2\tilde{\alpha}}^2)(1-c_{2c}^2)(1+s_b^4) + 4s_{2\tilde{\alpha}}\, c_{2c}\, s_{2c}\, s_b(1-3c_{2\tilde{\alpha}}^2)(1+s_b^2) \\ &+ 2c_{2\tilde{\alpha}}\, s_b^2[1-7c_{2c}^2 - 3c_{2\tilde{\alpha}}^2(1-3c_{2c}^2)] = 0, \\ &(1-c_{2\tilde{\alpha}}^2)(1-c_{2c}^2)(1-6s_b^6) + c_{2\tilde{\alpha}}\, s_{2\tilde{\alpha}}\, c_{2c}\, s_{2c}\, s_b(22s_b^4 + 8s_b^2 - 6) - 8s_b^2(1-c_{2\tilde{\alpha}}^2 c_{2c}^2) \end{aligned} \tag{A.7}$$

$$+ s_b^4[13 - 27c_{2\tilde{\alpha}}^2 c_{2c}^2 + 7(c_{2\tilde{\alpha}}^2 + c_{2c}^2)] = 0, \tag{A.8}$$

$$c_{2c}\,(1 - c_{2\tilde{\alpha}}^2)(1 - c_{2c}^2)(1 + s_b^4) + c_{2\tilde{\alpha}}\, s_{2\tilde{\alpha}}\, s_{2c}\, s_b(1 - 4c_{2c}^2)(1 + s_b^2)$$
$$- 2c_{2c}\, s_b^2[2c_{2\tilde{\alpha}}^2 + c_{2c}^2(1 - 3c_{2\tilde{\alpha}}^2)] = 0 \tag{A.9}$$

While these three equations are highly non-linear, the solution of interest is actually obtained quite simply by setting

$$c_{2\tilde{\alpha}} = 0, \quad c_{2c} = 0, \tag{A.10}$$

whereby Eqs. (A.7) and (A.9) become trivially satisfied, and Eq. (A.8) takes the simple form

$$6s_b^6 - 13s_b^4 + 8s_b^2 - 1 = 0, \tag{A.11}$$

the interesting solution of which is $s_b^2 = 1/6$.

Summarizing, the maxima are obtained for

$$\tilde{\alpha} = \pm\tfrac{1}{4}\pi, \qquad \alpha_b = \pm \arcsin\sqrt{\tfrac{1}{6}} = \pm 0.13386\pi \quad (24.1\,^\circ), \qquad \alpha_c = \pm\tfrac{1}{4}\pi, \tag{A.12}$$

at which point

$$z = \pm\frac{3125}{8 \times 1024 \times 27^2} \tag{A.13}$$

determines the γ_0 of (4.17).

References

[1] A. Mendez and A. Pomarol, Phys. Lett. B **272** (1991) 313.

[2] T. D. Lee, Phys. Rev. D **8** (1973) 1226;
G. C. Branco and M. N. Rebelo, Phys. Lett. B **160** (1985) 117;
J. Liu and L. Wolfenstein, Nucl. Phys. B **289** (1987) 1;
S. Weinberg, Phys. Rev. D **42** (1990) 860;
Y. L. Wu and L. Wolfenstein, Phys. Rev. Lett. **73** (1994) 1762 [arXiv:hep-ph/9409421].

[3] J.F. Gunion, H.E. Haber, G. Kane, S. Dawson, *The Higgs Hunter's Guide* (Addison-Wesley, Reading, 1990).

[4] I. F. Ginzburg, M. Krawczyk and P. Osland, arXiv:hep-ph/0101208;
Nucl. Instrum. Meth. A **472** (2001) 149 [arXiv:hep-ph/0101229];
arXiv:hep-ph/0211371;

[5] W. Khater and P. Osland, Nucl. Phys. **B**, in print, arXiv:hep-ph/0302004.

[6] I. F. Ginzburg, M. Krawczyk and P. Osland, preprint CERN-TH/2003-020, to be published.

[7] W. Bernreuther and A. Brandenburg, Phys. Rev. D **49** (1994) 4481 [arXiv:hep-ph/9312210].

[8] W. Bernreuther, A. Brandenburg and M. Flesch, CERN-TH/98-390, PITHA 98/41, arXiv:hep-ph/9812387.

[9] T. Hahn and M. Perez-Victoria, Comput. Phys. Commun. **118** (1999) 153 [arXiv:hep-ph/9807565]. See also http://www.feynarts.de/looptools/

[10] G. J. van Oldenborgh and J. A. Vermaseren, Z. Phys. C **46** (1990) 425.

[11] J. Pumplin, D. R. Stump, J. Huston, H. L. Lai, P. Nadolsky and W. K. Tung, JHEP **0207** (2002) 012 [arXiv:hep-ph/0201195].

[12] F. James and M. Roos, Comput. Phys. Commun. **10** (1975) 343.

[13] S. L. Glashow and S. Weinberg, Phys. Rev. D **15** (1977) 1958.

[14] G. C. Branco, L. Lavoura, J. P. Silva, "CP Violation" (Oxford Univ. Press, 1999).